Asian Journal of Chemistry; Vol. 33, No. 12 (2021), 3123-3128

ASIAN JOURNAL OF CHEMISTRY

https://doi.org/10.14233/ajchem.2021.23505

Catalytic Activity of Green Synthesized Silver Nanoparticles on Alkaline Hydrolysis of Crystal Violet Dye

SALIMA BEGUM and R.K. LONDON SINGH*

Department of Chemistry, D.M. College of Science, Dhanamanjuri University, Manipur-795001, India

*Corresponding author: E-mail: london_ningthemcha@yahoo.com

Received: 30 August 2021; *Accepted*: 16 October 2021; *Published online*: 6 December 2021; AJC-20608

Silver nanoparticles (AgNPs) were prepared by employing green chemicals such as gallic acid as reductant and starch as a stabilizer. The maximum absorption peak at 443 nm of the synthesized nanoparticles was observed in UV-visible spectrum. The existence of the fcc structure of silver nanocrystal with intense diffraction peak along (111) plane with a crystallite size of 9.32 ± 1.31 nm was evidenced from XRD studies. Quasi-spherical AgNPs of average diameter 48.42 ± 14 nm, hexagonal AgNPs with mean edge length 31.75 ± 7.29 nm and triangular AgNPs of mean edge length 48.55 ± 11.37 nm were confirmed from the TEM images. FTIR analysis verified that the synthesized AgNPs were stabilized by starch. The AgNPs was used as a catalyst in the alkaline hydrolysis of crystal violet dye. A 2.41×10^{-2} min^{-1} and 4.49×10^{-2} min^{-1} were degradation rate constants of crystal violet in the absence and presence of silver nanoparticles, respectively. The results clearly highlighted that the green synthesized silver nanoparticles can be used as catalyst in the degradation of toxic dyes in industrial effluents and environment.

Keywords: Silver nanoparticles, Gallic acid, Starch, Catalytic application, Crystal violet.

INTRODUCTION

Among the synthesized noble metal nanoparticles, silver nanoparticles (AgNPs) are more attracted than gold and palladium nanoparticles, because of its low cost, environment friendly, abundance, high photostability and catalytic properties [1-3]. It has better unique characteristics as compared to bulk form and hence, extensive studies on silver nanoparticles have been carried out and found applications in many fields. The bactericidal properties of silver nanoparticles have been cited in the literature [4-7]. The studies on the anticancer properties of AgNPs have also been well documented [8-10]. Silver nanoparticle synthesis using the green method is widely discussed because it reduced hazardous wastes to the environment and for safer clinical applications [11,12]. Synthesis of silver nanoparticles using green methods require environmentally friendly solvents and non-toxic chemicals [13-18].

Effective applications of silver nanoparticles dependent upon the sizes and shape. To tune the sizes of silver nanoparticles, various capping/stabilizing agents are used [19-22]. Green reducing agent like gallic acid which is a natural polyphenolic compound is used in AgNPs synthesis [23-25]. The designing of a fast, stable and simple method for AgNPs synthesis at room temperature in aqueous media is still a challenge. Therefore, fast synthesis of stable AgNPs at low pH using gallic acid as reductant and starch as a capping agent at room temperature is reported here. The crystallite size of the synthesized AgNPs was determined by using Debye-Scherrer's formula. TEM images revealed the existence of quasi-spherical, highly facet hexagonal and triangular silver nanoparticles. The synthesized AgNPs exhibited catalytic effect on the alkaline hydrolysis of crystal violet dye and its reaction rate increases 2.1 times. The method used to study catalytic activity here is simple, fast, cost-effective and reliable and can be used for scavenging of toxic dyes from the contaminated samples.

EXPERIMENTAL

Silver nitrate, gallic acid and starch were procured from Sigma-Aldrich, USA. Analytical grade sodium hydroxide was also purchased from Merck. Crystal violet dye was purchased from Himedia. Aqua-regia solution was used for cleaning all the glasswares and finally rinsed with deionized water.

Synthesis of AgNPs: In a cleaned 150 mL beaker, 20 mL of $AgNO_3$ (50 mM) was mixed with 50 mL of starch (0.34% w/v) and stirred for 3 min at 25 ºC using a magnetic stirrer. To the above solution, 30 mL of gallic acid (50 mM) was added quickly and mixed thoroughly for another 2 min. One drop (0.05 mL) of NaOH (0.1 M) was added to the above mixture and immediately recorded the time of the start of the reaction by using a stopwatch. The pH of the above mixture was noted by using a pH-meter (Systronic pH System 361). The solution colour becomes light yellow and then to deep grey within a few seconds. The stirring of the solution continued for another 3 min for the homogeneous mixing of the solution. For examining of nanoparticle formation and its stability, the absorbance was measured at 3 min, 18 min, 60 min, 84 min, 1 d, 3 d, 5 d, 9 d and 52 d by taking 0.1 mL of the reaction mixture and diluting it with 4 mL of deionized water in a quartz cuvette by using Beckman Coulter DU 720 spectrophotometer in the scan range of 300-700 nm. The obtained AgNPs colloidal solution was purified repeatedly by centrifugation for 10 min using REMI R-24 at 10,000 rpm followed by re-dispersion of the residue in deionized water and this process was repeated for three times. Finally, at room temperature, the purified AgNPs pellets were dried and kept in an Amber bottle for characterization and applications. The mechanism of the reaction is given in Fig. 1.

Characterization of AgNPs: The maximum absorption band of the synthesized nanoparticles was recorded by using a UV-Vis spectrophotometer (Beckman Coulter DU 720 Spectrophotometer) at room temperature. Powder X-ray diffractogram of the prepared sample was taken by using BRUKER D2 phase diffractometer (Cu*K*α, λ = 1.54182 Å, 30 kV) in the scan range 2θ = 20-80º by preparing a thin film of the silver nanoparticles on a clean commercial glass slide. The phase composition and crystallite size were calculated from the XRD data by analyzing the X-ray diffractogram by using Origin software. The particle sizes of the prepared nanoparticles were measured by employing transmission electron microscopy (JEM-2100, Jeol, 200 kV). The FTIR spectroscopy of AgNP was carried out by using the FTIR spectrophotometer (Tensor 27, Bruker, equipped with ZnSe ATR) in the range of 4000-500 cm^{-1}, whereas the surface morphology was analyzed by using FESEM, SUPRA55 (CARL ZEISS, Germany).

Catalytic degradation: The catalytic activity of the synthesized AgNPs on alkaline hydrolysis of crystal violet dye was carried out at room temperature. Firstly, maximum absorbance (λ_{max}) of crystal violet solution made by mixing 6 mL deionized water with 4 mL dye (1×10^{-4} M) was recorded by using Beckman Coulter DU 720 spectrophotometer. Secondly, a control was prepared by mixing 5 mL deionized water with 4 mL crystal violet dye (1×10^{-4} M) and 1 mL of NaOH (5×10^{-2} M) solution. The absorbance maxima of the control were monitored by using UV-Vis spectrophotometer at different time intervals. Thirdly, 4.9 mL deionized water, 4 mL crystal violet dye (1×10^{-4} M), 1 mL NaOH (5×10^{-2} M) and 0.1 mL prepared colloidal AgNPs were mixed and measured its absorbance maxima at different time intervals. The total volume of every mixture was fixed at 10 mL and reaction time at 20 min. The degradation percentage was determined by using eqn. 1:

$$\text{Degradation (\%)} = \frac{A_o - A}{A_o} \times 100 \quad (1)$$

where A_o and A are the absorbances of crystal violet dye solution at times corresponding to 0 min and t min, respectively, at a characteristic absorption wavelength of 590 nm. Langmuir-Hinshelwood equation was used for the study of the kinetics of degradation, which is expressed by eqn. 2 [26]:

$$\ln\left(\frac{A}{A_o}\right) = -kt \quad (2)$$

The slope of straight-line plot of ln (A/A_0) *vs.* degradation time, t gives the pseudo-first-order rate constant, k of the reaction.

RESULTS AND DISCUSSION

UV-visible studies: UV-vis spectra of AgNPs formed by reducing silver nitrate with gallic acid and stabilized with starch is shown in Fig. 2. There is no detectable surface plasmon resonance (SPR) band before 3 min of reaction time indicating that there is no formation of a sufficient amount of AgNPs. But, after 3 min, silver nanoparticles formation started with changing colour from light yellow to dark brown with a characteristic surface plasmon resonance bands [27-29]. The maximum absorption bands of the nanoparticles exhibited a bathochromic shift with the progress of reaction time starting from 419 nm and remained constant at 444 nm after 24 h. This might be due to the slight AgNPs agglomeration with long storage time. The colour of the synthesized nanoparticles did not show any significant change in colour over 52 days which supports the stability of the synthesized AgNPs [30].

XRD studies: The XRD pattern of the prepared AgNPs along with JCPDS File No. 04-0783 is shown in Fig. 3. There

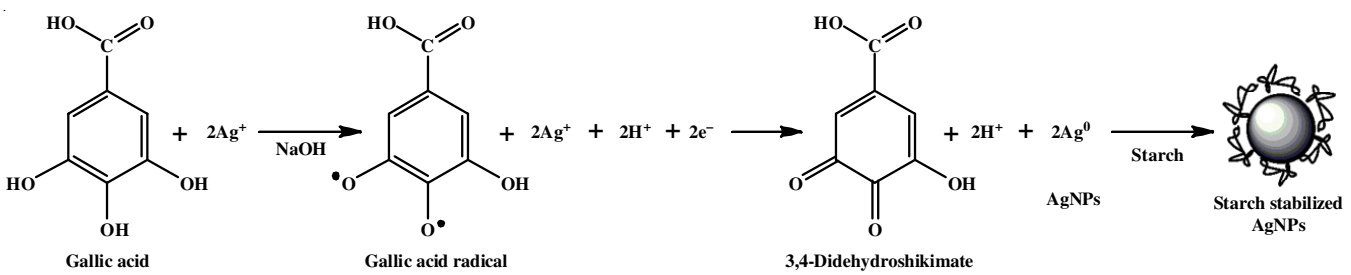

Fig. 1. Schematic representation of the reaction mechanism of the formation of silver nanoparticles using gallic acid as reducing agent and starch as the stabilizing agent

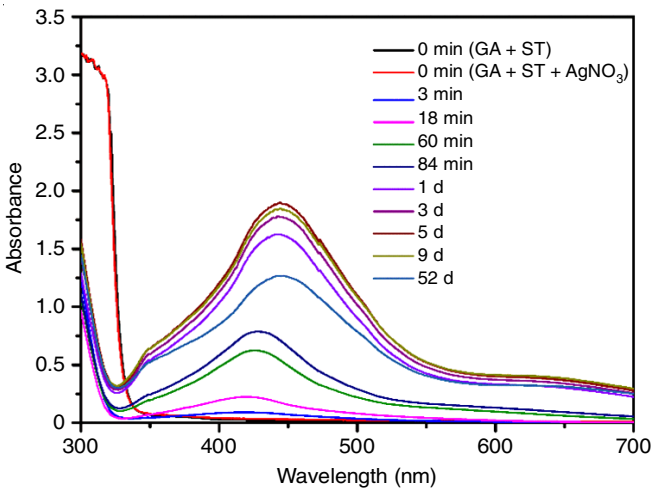

Fig. 2. UV-vis spectra of silver nanoparticles synthesized by using gallic acid as reducing agent and starch as the stabilising agent

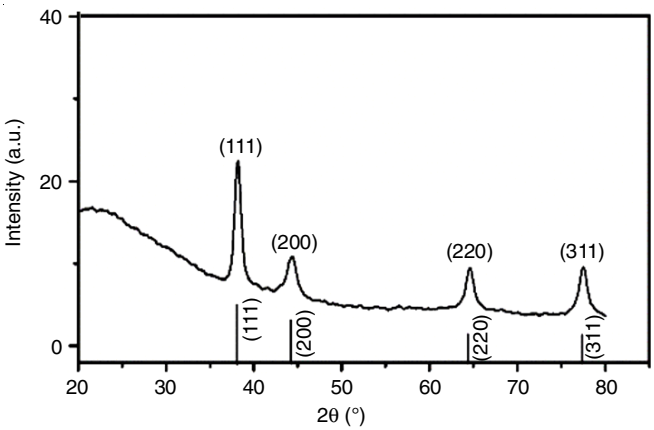

Fig. 3. XRD spectrum of synthesized silver nanoparticles

are no extra peaks due to the presence of impurities in the diffractogram. The highest intense peak is along the (111) plane. The high intensity of peaks attributes to a high degree of crystallinity of AgNPs. The broad nature of the peaks indicates the polydisperse nature of the synthesized silver nanoparticles [31]. The peaks at 2θ values 38.018º, 44.289º, 64.396º and 77.452º are assigned to (111), (200), (220) and (311) planes, respectively of the fcc structure of silver and the diffraction pattern is well-matched with JCPDS File No. 04-0783 of the fcc crystal structure of silver. The average crystallite size of the nanoparticle was calculated by using Debye-Scherrer's formula [32] ($D = K\lambda/(\beta\cos\theta)$), where, D is average crystallite size, K = 0.94, $\lambda = 0.154$ nm is the wavelength of X-ray reflection, full-width at half maximum (FWHM) of the XRD peaks was measured in radian and is represented by β. The average crystallite size calculated using the above formula was found to be 9.324 ± 1.314 nm.

Morphology studies: The TEM micrographs of the synthesized AgNPs are shown in Fig. 4a-b with 200 nm and 100 nm scale bars, respectively. It is seen from the TEM images that the synthesized AgNPs consists of quasi-spherical silver nanoparticles of average diameter 48.42 ± 14 nm, highly facet hexagonal silver nanoparticles with a mean edge length 31.75 ± 7.29 nm and triangular silver nanoparticles of mean edge length 48.55 ± 11.37 nm. It is also observed from the TEM micrographs that the population of quasi-spherical silver nanoparticles is more dominant than hexagonal and triangular AgNPs. Selected-area electron diffraction patterns of AgNPs is shown in Fig. 4c and the presence of bright circular spots confirmed the existence of crystalline silver nanoparticles [33].

Fig. 5a-c show the histograms showing the size distributions of AgNPs of quasi-spherical, hexagonal and triangular silver nanoparticles, respectively. Fig. 6 shows the scanning electron micrographs of the as-formed silver nanoparticles and revealed the surface morphology of the synthesized AgNPs and indicating a uniform distribution of the nanoparticles.

FTIR studies: Fig. 7a shows the FTIR spectra of the synthesized AgNPs stabilized with (0.34 w/v) starch and pure starch (Fig. 7b) at room temperature. A strong O-H stretching band of starch is observed at 3308 cm^{-1}. An asymmetric stretching band due to C-H is observed at 2958 cm^{-1}. The strong absorption band at 1635 cm^{-1} is due to the O-H bending of water adsorbed in starch. Intra and intermolecular hydrogen bonding are responsible for slight shifting of band observed in 3309-3308 cm^{-1} in AgNPs. The binding of OH group of starch to AgNPs is confirmed by the observance of characteristic bands of starch [34].

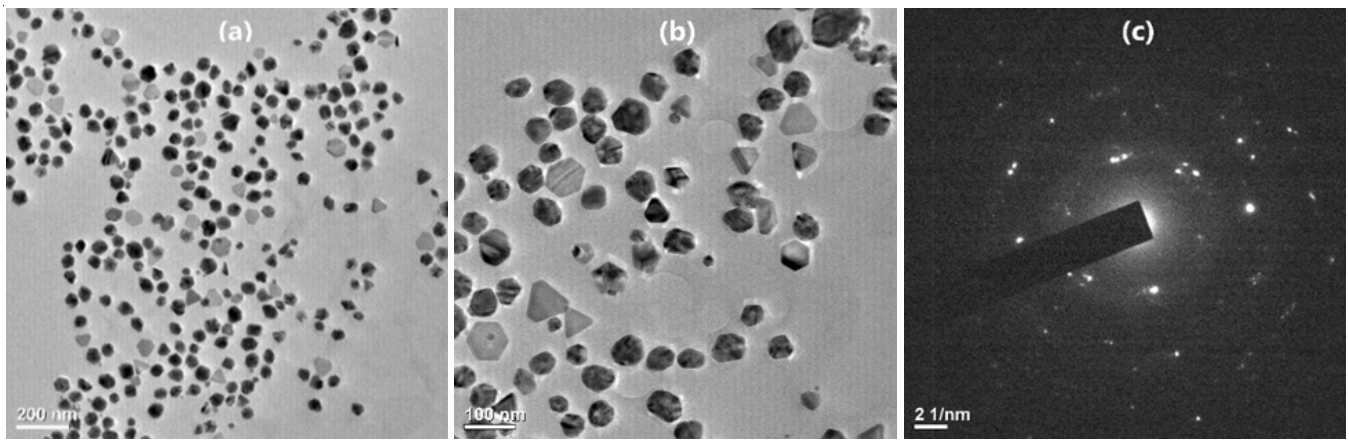

Fig. 4. (a) TEM micrograph of synthesized AgNPs (scale bar = 200 nm); (b) TEM micrograph of synthesized AgNPs (Scale bar = 100 nm); (c) SAED pattern of AgNPs

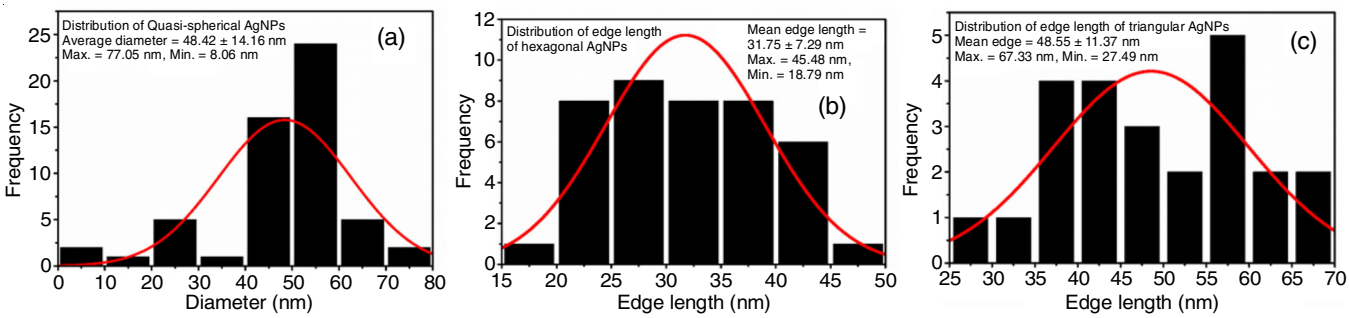

Fig. 5. Histogram showing size distributions of AgNPs (a) quasi-spherical, (b) hexagonal and (c) triangular AgNPs

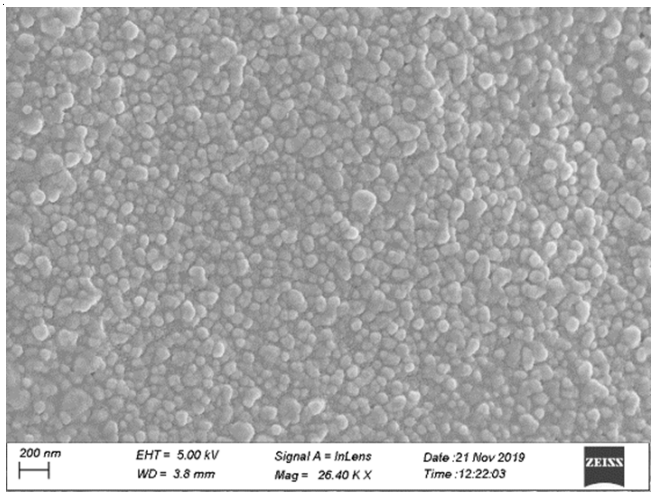

Fig. 6. SEM micrograph of synthesized AgNPs

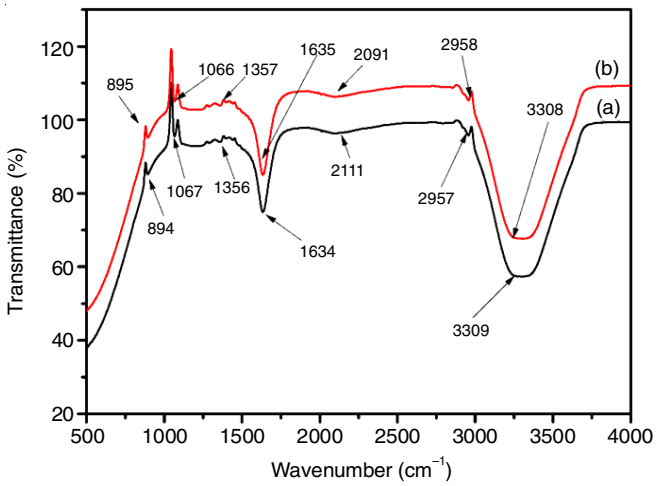

Fig. 7. FTIR spectra of (a) starch stabilized AgNPs (b) pure starch

Catalytic effect of AgNPs on alkaline hydrolysis of crystal violet dye: The λ_{max} of crystal violet dye in aqueous solution shows an absorption band at 590 nm. Plots of relative absorption band *versus* absorption intensity as a function of time in the absence of AgNPs is shown in Fig. 8a and whereas in the presence of AgNPs is shown in Fig. 8b. A decrease in the absorption intensity with time is due to the formation of triarylleucohydroxide, a colourless product (Fig. 9).

Fig. 10a and 10b are the straight-line plots drawn between Ln (A/A_o) *vs.* time in the absence and presence of AgNPs, respectively. Table-1 shows the degradation percentage (D %) of crystal violet in the absence and presence of AgNPs, the ratio of degradation percentage and the average ratio of degradation percentage. From Table-1, the degradation percentage ratio is 1.5 and almost uniform throughout the reaction, which attributes to the uniform catalytic function of synthesized AgNPs. From the slopes of straight-line plots, the degradation reaction rate constants were also calculated and found to be 2.41×10^{-2} min^{-1} and 4.49×10^{-2} min^{-1}, in the absence and the presence of AgNPs, respectively. From the rate constant values, it was found

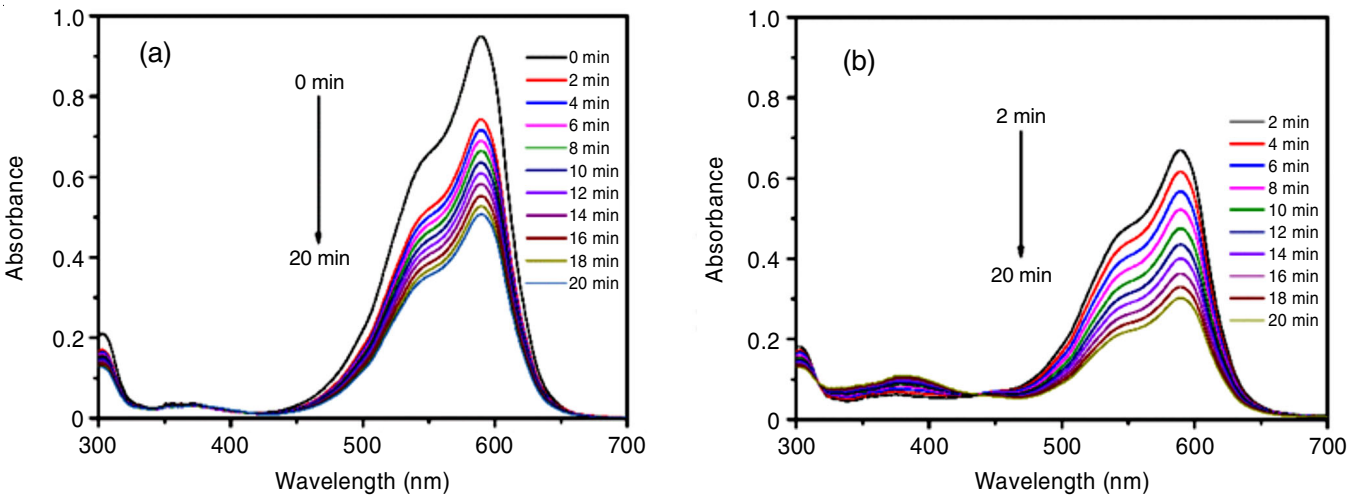

Fig. 8. Catalytic degradation of crystal violet using synthesized AgNP (a) in absence of AgNPs (b) in presence of AgNPs

TABLE-1
DEGRADATION PERCENTAGE (D, %) OF CRYSTAL VIOLET IN THE ABSENCE AND PRESENCE OF AgNPs, THE RATIO OF D (%) AND THE AVERAGE RATIO OF D (%)

Time (min)	Absence of AgNPs		Presence of AgNPs		Ratio of D (%)	Average ratio of D (%)
	Absorbance	D (%)	Absorbance	D (%)		
0	0.95	–	0.95	–	–	
2	0.74	22.11	0.67	29.47	1.3	
4	0.72	24.21	0.62	34.74	1.4	
6	0.69	27.37	0.57	40.00	1.5	
8	0.66	30.53	0.52	45.26	1.5	
10	0.64	32.63	0.48	49.47	1.5	1.5
12	0.61	35.79	0.44	53.68	1.5	
14	0.58	38.95	0.4	57.89	1.5	
16	0.55	42.11	0.36	62.11	1.5	
18	0.53	44.21	0.33	65.26	1.5	
20	0.51	46.32	0.3	68.42	1.5	

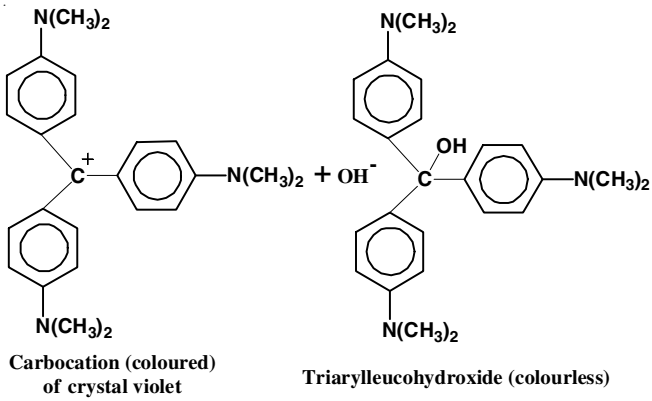

Fig. 9. Alkaline hydrolysis of crystal violet and formation of triarylleucohydrooxide (a colourless product)

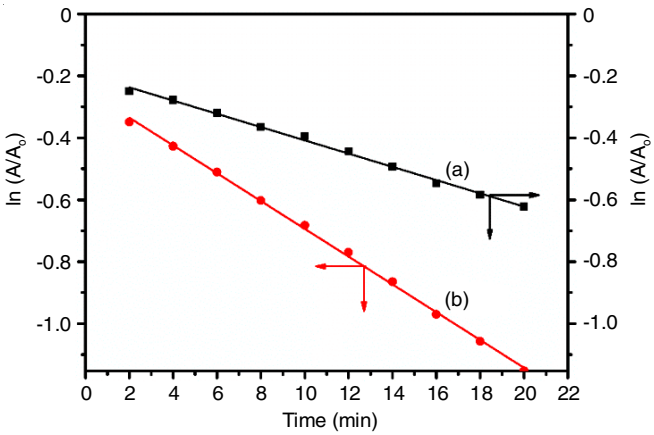

Fig. 10. Linear plot of ln (A/A_0) *vs.* t of crystal violet degradation

that the reaction rate of alkaline hydrolysis of crystal violet dye is 2.1 times enhanced due to the presence of AgNPs. The synthesized AgNPs helps the electron relay from OH^- to crystal violet dye (acceptor). The OH^- ions are nucleophilic, while crystal violet is electrophilic concerning AgNPs, where the AgNPs accept electrons from OH^- ions and convey them to crystal violet forming the colourless product [35].

Conclusion

Successfully synthesized quasi-spherical, hexagonal and triangular AgNPs using green chemicals, starch and gallic acid at room temperature (25 ºC). The XRD analysis revealed the formation of face centre cubic structure of silver crystal with preferential orientation along (111) plane with a crystallite size of 9.32 ± 1.31 nm. TEM images showed the formation of quasi-spherical, highly facet hexagonal and triangular silver nanoparticles. The average degradation percentage was 1.5 and the catalytic action of the synthesized AgNPs was uniform throughout the reaction. The reaction rate of degradation of crystal violet dye in alkaline medium was increased by 2.1 times due to the presence of AgNPs. These experimental findings will have the potential applications in removing the toxic dyes from industrial effluents.

ACKNOWLEDGEMENTS

The authors are thankful to the Sophisticated Analytical Instrument Facility (SAIF), Shillong, Department of Physics, Tripura University, Tripura and National Institute of Technology, Imphal, India for extending their technical support and assistance in the characterization of the synthesized silver nanoparticles.

CONFLICT OF INTEREST

The authors declare that there is no conflict of interests regarding the publication of this article.

REFERENCES

1. W. Lu, X. Qin, H. Li, A.M. Asiri, O. Al-Youbi and X. Sun, *Part. Part. Syst. Charact.*, **30**, 67 (2013); https://doi.org/10.1002/ppsc.201200033
2. D. Yu and V.W.-W. Yam, *J. Am. Chem. Soc.*, **126**, 13200 (2004); https://doi.org/10.1021/ja046037r
3. M. Rashid and T. Mandal, *J. Phys. Chem. C*, **111**, 16750 (2007); https://doi.org/10.1021/jp074963x
4. G. Guzmán, J. Dille and S. Godet, *Nanomed-Nanotechnol.*, **8**, 37 (2012); https://doi.org/10.1016/j.nano.2011.05.007
5. V.K. Sharma, R.A. Yngard and Y. Lin, *Adv. Colloid Interface Sci.*, **145**, 83 (2009); https://doi.org/10.1016/j.cis.2008.09.002
6. S.M. Lee, K.C. Song and B.S. Lee, *Korean J. Chem. Eng.*, **27**, 688 (2010); https://doi.org/10.1007/s11814-010-0067-0
7. G.A. Martínez-Castañón, N. Niño-Martínez, F. Martínez-Gutierrez, J.R. Martínez-Mendoza and F. Ruiz, *J. Nanopart. Res.*, **10**, 1343 (2008); https://doi.org/10.1007/s11051-008-9428-6
8. W.I. Abdel Fattah and G.W. Ali, *J. Appl. Biotechnol. Bioeng.*, **5**, 43 (2018); https://doi.org/10.15406/jabb.2018.05.00116

9. M. Jeyaraj, G. Sathishkumar, G. Sivanandhan, D. Mubarak Ali, M. Rajesh, R. Arun, G. Kapildev, M. Manickavasagam, N. Thajuddin, K. Premkumar and A. Ganapathi, *Colloids Surf. B Biointerfaces*, **106**, 86 (2013); https://doi.org/10.1016/j.colsurfb.2013.01.027
10. M. Morais, V. Machado, F. Dias, C. Palmeira, G. Martins, M. Fonseca, C.S.M. Martins, A.L. Teixeira, J.A.V. Prior and R. Medeiros, *Nanomaterials*, **11**, 256 (2021); https://doi.org/10.3390/nano11020256
11. J.E. Hutchison, *ACS Nano*, **2**, 395 (2008); https://doi.org/10.1021/nn800131j
12. J.A. Dahl, B.L.S. Maddux and J.E. Hutchison, *Rev.*, **107**, 2228 (2007); https://doi.org/10.1021/cr050943k
13. M. Shu, F. He, Z. Li, X. Zhu, Y. Ma, Z. Zhou, Z. Yang, F. Gao and M. Zeng, *Nanoscale Res. Lett.*, **15**, 14 (2020); https://doi.org/10.1186/s11671-019-3244-z
14. Z. Khan, J.I. Hussain, S. Kumar, A.A. Hashmi and M.A. Malik, *J. Biomater. Nanobiotechnol.*, **2**, 390 (2011); https://doi.org/10.4236/jbnb.2011.24048
15. Z. Yi, X. Li, X. Xu, B. Luo, J. Luo, W. Wu, Y. Yi and Y. Tang, *Colloids Surf. A Physicochem. Eng. Asp.*, **392**, 131 (2011); https://doi.org/10.1016/j.colsurfa.2011.09.045
16. M. Venkatesham, D. Ayodhya, A. Madhusudhan, N. Veera Babu and G. Veerabhadram, *Appl. Nanosci.*, **4**, 113 (2014); https://doi.org/10.1007/s13204-012-0180-y
17. S. Srikar, D. Giri, D. Pal, P. Mishra and S. Upadhyay, *Green Sustain. Chem.*, **6**, 34 (2016); https://doi.org/10.4236/gsc.2016.61004
18. S. Wei, Y. Wang, Z. Tang, J. Hu, R. Su, J. Lin, T. Zhou, H. Guo, N. Wang and R. Xu, *New J. Chem.*, **44**, 9304 (2020); https://doi.org/10.1039/D0NJ01335H
19. J. Tashkhourian and O. Sheydaei, *Anal. Bioanal. Chem. Res.*, **4**, 249 (2017); https://doi.org/10.22036/abcr.2017.69942.1127
20. P. Vasileva, T. Alexandrova and I. Karadjova, *J. Chem.*, **2017**, 1 (2017); https://doi.org/10.1155/2017/6897960
21. K. Praveenkumar, M.K. Rabinal, M.N. Kalasad, T. Sankarappa and M.D. Bedre, *IOSR J. Appl. Phys.*, **5**, 43 (2014); https://doi.org/10.9790/4861-0554351
22. C.M. Phan and H.M. Nguyen, *J. Phys. Chem. A*, **121**, 3213 (2017); https://doi.org/10.1021/acs.jpca.7b02186
23. D. Li, Z. Liu, Y. Yuan, Y. Liu and F. Niu, *Process Biochem.*, **50**, 357 (2015); https://doi.org/10.1016/j.procbio.2015.01.002
24. A.K. Mittal, S. Kumar and U.C. Banerjee, *J. Colloid Interface Sci.*, **431**, 194 (2014); https://doi.org/10.1016/j.jcis.2014.06.030
25. S.N. Sunil Gowda, S. Rajasowmiya, V. Vadivel, S.B. Devi, A.C. Jerald, S. Marimuthu and N. Devipriya, *Toxicol. Vitr.*, **52**, 170 (2018); https://doi.org/10.1016/j.tiv.2018.06.015
26. A. Nezamzadeh-Ejhieh and H. Zabihi-Mobarakeh, *J. Ind. Eng. Chem.*, **20**, 1421 (2014); https://doi.org/10.1016/j.jiec.2013.07.027
27. P. Mulvaney, *Langmuir*, **12**, 788 (1996); https://doi.org/10.1021/la9502711
28. M. Yilmaz, H. Turkdemir, M.A. Kilic, E. Bayram, A. Cicek, A. Mete and B. Ulug, *Mater. Chem. Phys.*, **130**, 1195 (2011); https://doi.org/10.1016/j.matchemphys.2011.08.068
29. V.S. Kotakadi, S.A. Gaddam, S.K. Venkata and D.V.R. Sai Gopal, *Appl. Nanosci.*, **5**, 847 (2015); https://doi.org/10.1007/s13204-014-0381-7
30. K. Barman, D. Chowdhury and P.K. Baruah, *Inorg. Nano-metal Chem.*, **50**, 57 (2020); https://doi.org/10.1080/24701556.2019.1661468
31. T. Devi, N. Ananthi and T. Amaladhas, *J. Nanostruc. Chem.*, **6**, 75 (2016); https://doi.org/10.1007/s40097-015-0180-z
32. A.I. Patterson, *Phys. Rev.*, **56**, 978 (1939); https://doi.org/10.1103/PhysRev.56.978
33. K. Jyoti, M. Baunthiyal and A. Singh, *J. Radiation Res. Appl. Sci.*, **9**, 217 (2016); https://doi.org/10.1016/j.jrras.2015.10.002
34. P. Sibiya, T. Xaba and M. Moloto, *Pure Appl. Chem.*, **88**, 61 (2016); https://doi.org/10.1515/pac-2015-0704
35. B. Ganapuram, M. Alle, R. Dadigala, A. Dasari, V. Maragoni and V. Guttena, *Int. Nano Lett.*, **5**, 215 (2015); https://doi.org/10.1007/s40089-015-0158-3